

Correlated mechanical microscopy with both EDS and EBSD for complex microstructures

Correlated mechanical microscopy is a powerful technique for materials science investigations. By correlating indentation properties maps with orientation maps obtained by energy-dispersive spectroscopy (EDS), composition-property relationships can be extracted. By correlating indentation properties maps with orientation maps obtained by electron back-scattered diffraction (EBSD), orientation-property relationships can be extracted. In this application note, an approach for performing correlative mechanical microscopy using both EDS and EBSD is outlined and demonstrated on a meteorite fragment. Using displacement-controlled indentations allowed consistent sampling from both mechanical, EDS, and EBSD sampled volumes. This demonstrates the potential of this correlative approach for complex microstructures.

Author: Dr. Jeffrey M. Wheeler

OXFORD
INSTRUMENTS

Introduction

In previous applications notes, we have demonstrated correlated mechanical microscopy with both energy-dispersive spectroscopy (EDS) and electron back-scattered diffraction (EBSD) separately. The combination of these techniques provides incredible insight into the relationships between mechanical properties, composition, and crystallographic phase and orientation. Their mutual micrometric length scale allows them to locally interrogate with high spatial resolution. However, correlation with each of these techniques presents distinct challenges.

Correlated mechanical microscopy with EDS can be performed in a relatively straightforward manner by simply performing a nanoindentation map, and then performing an EDS map on the same region with matching resolution. As the nanoindentation deformation does not change the local composition, the EDS mapping can easily be done after the indentation map using the indentation grid as a fiducial for alignment. This provides an ideal 1:1 correlation between the two

datasets, as previously demonstrated in a combinatorial investigation of the Ni—Ta system [1].

Correlating mechanical microscopy with EBSD is more challenging due to two factors. Alignment is more challenging due to the 70° tilted orientation of the sample required in the scanning electron microscope (SEM) for EBSD acquisition. Further, EBSD should ideally be performed before the nanoindentation map, as the indentation process produces surface deformation which might affect the EBSD pattern quality. Therefore, additional fiducial markings are required to facilitate alignment of the two grids. However, some distortion of the data matrices is likely to occur due to the angular tilt mentioned above, requiring an affine transformation and interpolation of the datasets to achieve correlation [2].

In this application note, nanoindentation, EDS and EBSD mapping are used to perform correlative mechanical microscopy on a fragment of the Seymchan meteorite. Meteorites often feature complex microstructures featuring compositional gradients and multiple phases. Correlative techniques are very important for data analysis to identify trends between the compositional and mechanical techniques, as analysis of one technique alone may be insufficient for data segmentation or deconvolution of overlapping clusters [3]. Details of the approach are described, particularly the system concerns, and the ability of the correlative approach to identify individual orientations and phases is demonstrated and discussed.

Experimental Considerations

To perform correlative mechanical microscopy, the sampled volumes measured by both techniques need to be similarly and regularly sized. For nanoindentation, this means that testing should be performed under displacement control, so that every indentation is made to the same maximum depth regardless of that phase's or orientation's properties. This aids in achieving a point-to-point correlation, which requires additional consideration.

Displacement Control

Displacement-controlled indentation mapping is highly preferable for correlative applications. In load control, the load must be carefully chosen to ensure that the spacing is proportional to the indentation produced in the softest phase in the map. Otherwise, indentations in the soft region will overlap with its neighbors. This means for indentations maps performed in load control, a significant disparity in indentations depths and spacings can be expected for maps over dissimilar phases.

In displacement control, indentations are all performed to the same maximum depth, ensuring similar indentation sizes and regular with minor variations from differences in elastic recovery. This is important for correlative measurements, so that every mechanical and analytical measurement is taken from the same volume of material.

Experimental Procedures

The Seymchan meteorite (Fe-9Ni-0.5Co) sample was extracted with a size of about

1×1×0.5 cm³, respectively, by electrical discharge machining or with a diamond saw. A metallographic preparation was then carried out to ensure an appropriately flat and deformation-free surface suitable for both, combined EDS-EBSD and nano-indentation experiments. Initially, the samples were mechanically ground and then polished using water-based diamond suspensions of progressively increasing fineness to a final 1 μm particle size. In order to minimize the surface relief, a short final mechanical polishing was performed with 0.25 μm colloidal silica (OP-S, Struers, Denmark) on a neoprene polishing cloth (OP-Chem, Struers).

Microstructural analyses were performed using analytical SEM, backscattered electron (BSE) imaging, and combined EDS-EBSD mapping in a dual-beam focused ion beam (FIB)-SEM Thermo Fisher Scientific Helios Nanolab 600i (Hikari, EDAX Inc.) and a Hitachi SU-5000 (Oxford UltimMax 100 EDS) at 20 kV. They were recorded with a step size of 1.3 μm across an area of 702×525 μm² for the steel and 1 μm step size across an 1280×769 μm² area for the Seymchan meteorite and were analyzed using the EDAX OIM 7.3.1 software as well as the free MTEX 5.7.0 toolbox based on Matlab® [4]. The EDS mapping results were later quantified by the EDAX TEAM software using the e-ZAF method with binning.

Nanoindentation mapping was performed using a FT-I04 Femto-Indenter (FemtoTools AG, Switzerland) equipped with an FT-S20,000 sensor and a diamond Berkovich tip. Each indentation was performed using continuous stiffness measurement (CSM) method [5] in displacement control. An oscillation frequency of 150 Hz and a proportionally scaled amplitude that linearly increased from 0.5 to 2.5 nm with increasing depth was used. A map of 384×216 indentations was performed with a maximum depth of 190 nm and a 2 μm spacing. This ensured an indentation depth/spacing ratio of 10 was maintained [6]. Representative values for each indentation were determined from the mean of values measured at contact depths above 50% of the target depth for elastic modulus and 80% for hardness to minimize errors from indentation size effects.

Results and Discussion

Correlated Maps

The Seymchan meteorite sample was used in order to demonstrate the combined capabilities of correlated mechanical microscopy. A Plessite region was selected for investigation, as it is comprised of a fine mixture of body-centered-cubic Kamacite (referred to hereafter as α) and thin seams of Taenite/Tetrataenite (referred to hereafter as γ) around the α grains. In addition, fine-grained intermediate domains of α and γ are visible. Figure 1 shows the results of the correlated mechanical microscopy study with aligned nanoindentation property, EDS, and EBSD maps and a BSE micrograph of the mapped region.

Several general trends between the phases are clear on first examination. The thin γ regions between the larger α grains in the Plessite region display simultaneously the highest hardness and lowest reduced modulus values. These regions correspond to the highest Nickel concentrations are often not well indexed by EBSD to a particular orientation, possibly due to a fine grain size. In general, a strong visual correlation can be noted between the regions with lower reduced modulus and the regions with high Nickel concentrations.

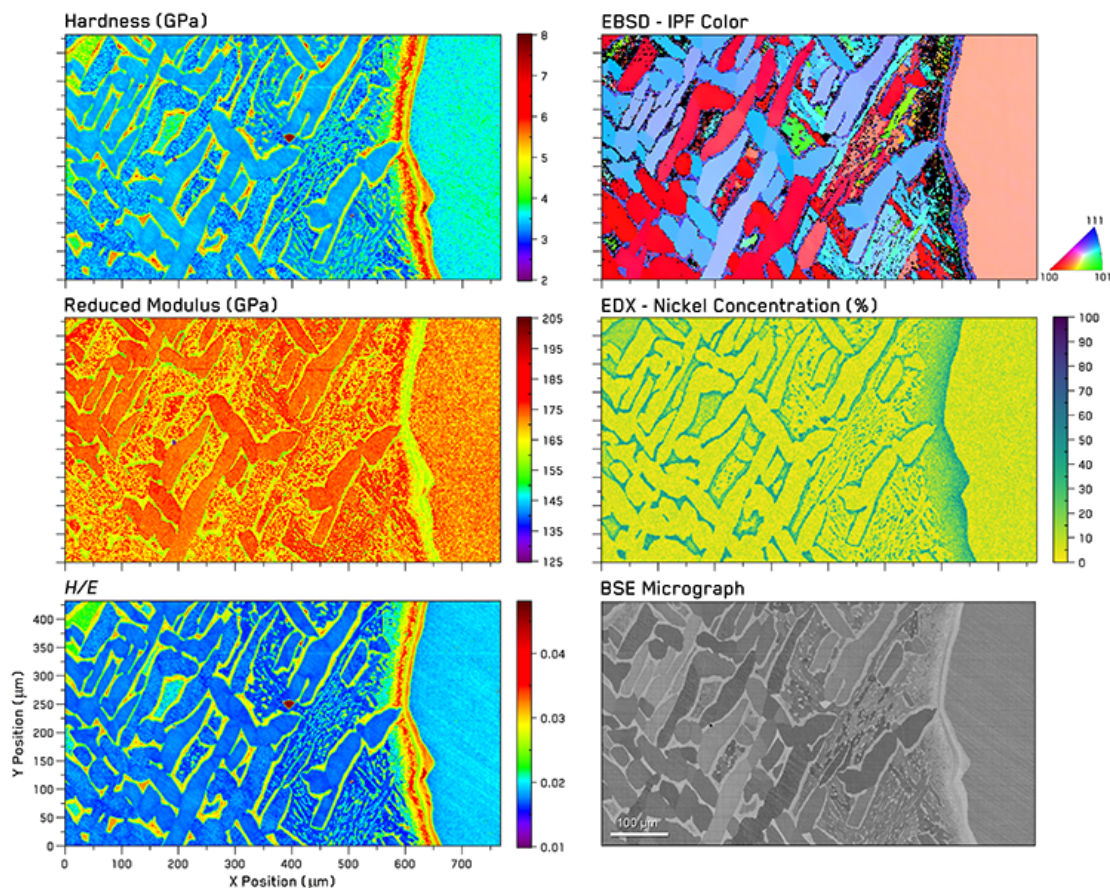


Figure 1. Mechanical microscopy results from the Seymchan meteorite with correlated indentation property maps with EBSD orientation, EDS Nickel concentration, and backscattered electron micrographs of the same region.

The α -phase regions can be considered separately as three different classes. The first being the largest α grain on the far right of the image, which is bordered by a large compositional gradient of high nickel concentration.

The second class of α grains show a similar range of orientations, light blue/purple in the EBSD map with inverse pole figure (IPF) coloring, relatively near to the [111] direction. These grains all show relatively consistent indentation properties throughout without much internal scatter in hardness or reduced modulus.

The last class of α grains are those oriented near to the [100] direction, shown in red in the IPF map. These grains show a much higher amount of variation in hardness and reduced modulus, resembling regions where fine γ -phase regions have precipitated. However, the γ phase precipitates do not appear in either EBSD or EDS maps or the BSE micrograph. This suggests that the precipitates might be sub-micron sized, though their mechanical effects are exerted on a much larger scale.

Another small precipitate phase notable in the indentation property maps is a very high hardness Schreibersite, $(\text{Fe,Ni})_3\text{P}$ phase near the center of the hardness map. As noted in another work [8], Schreibersite displays very similar modulus to α Kamacite despite its high hardness. This was identified in EDS maps of P concentration, but these are not shown here.

The compositional gradient at the border of the large Kamacite grain at the far right of the region warrants some additional discussion. This feature forms as Nickel is

rejected from the α phase grain, generating a high Ni concentrate at the border which decreases with distance. This is very similar to compositional gradients observed at the borders of large α Kamacite bands in a Taza meteorite fragment previously [8]. At near equiatomic Fe and Ni concentrations, the Tetrataenite, FeNi¹⁰⁰, phase forms which has high hardness and lower modulus compared to Kamacite. This forms a distinct band within the gradient. Then as the Ni concentration decreases, a nanocomposite Cloudy Zone region of very high hardness forms which consists of Tetrataenite in a Taenite matrix, which is difficult for EBSD to index. Finally, the Ni concentration decreases to the point where the Ni-rich precipitates are fully segregated into coarser-grained regions forming the Plessite phase.

3.2. Correlated Property Distributions

Visual correlation of the salient features in the different characterization modalities (nanoindentation, EDS, and EBSD) can provide insights into specific microstructural features. However, to extract statistical trends from these maps, it is useful to look at them as a 2D histogram (Figure 2), which provides a visual representation of major statistical clusters. In this plot, we can clearly identify three major clusters. The hardest of these is easily attributed to the tetrataenite γ phase, but the two lower clusters are more challenging to attribute to specific phases/regions beyond likely being α Kamacite.

To characterize the nature of these clusters, it is helpful to use correlated results from EDS and EBSD, as shown in the color coded 2D scatter plots in Figure 2. By examining these plots, several features become clear. The hardest cluster is confirmed as the tetrataenite γ phase with orientations near [111] and the highest Ni at. % concentrations, and this cluster also contains the majority of points which were not indexed (black) by EBSD. This makes sense as these Tetrataenite bands are the finest scale features in the map, which likely contain multiple phases under indentations of this size, preventing easy indexing.

Next, the two 2D histogram clusters attributed to α Kamacite are indeed Kamacite. The cluster with the higher hardness of these is shown to be large Kamacite band at the far right of the map. Whereas the wide cluster with lower hardness is revealed to consist of two clusters, corresponding to the two orientations of larger, elongated grains in the Plessite region. The smaller of these clusters, in light blue/purple, consists of the grains where relatively uniform, smooth properties were observed. While the larger cluster oriented near [100] shows a wide scatter in properties, likely due to the significant amounts of precipitate phases inside those grains. This is also suggested by the higher Ni concentration datapoints observed scattered within this cluster, but this might also be due to mis-indexing at indentations which traverse interfaces.

3.3. Correlation Challenges

While this investigation in correlated mechanical microscopy was successful in identifying the major phases within the Seymchan meteorite fragment, it also reveals some challenges that the correlated approach highlights. In general, correlation can be challenging if there is insufficient statistical data or if there are features within the dataset that reduce alignment precision, such as noise within the data, complex grain boundary regions, and microstructures featuring multiple length scales. While

this dataset certainly included sufficient statistical data, the latter complications are notable within the data.

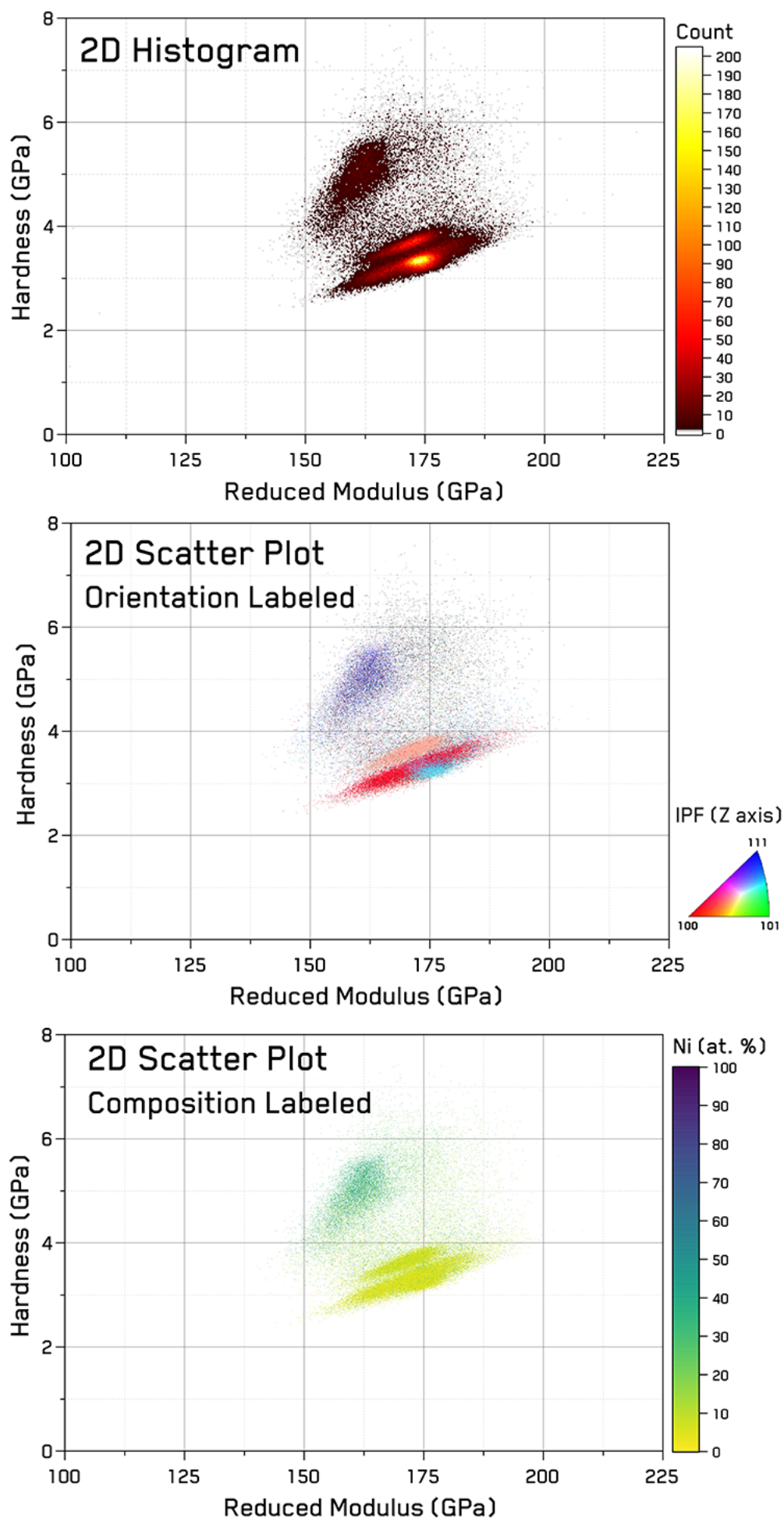


Figure 2. Statistics of correlated mechanical property distributions: 2D histogram of hardness vs

reduced modulus and 2D scatter plots with datapoints color coded using correlated EDS and EBSD data.

Addressing these challenges can be accomplished using a number of different tactics. Longer dwell times can be used to improve the precision of the EDS maps. Higher resolution maps can be performed to address length scale issues and issues with indexing EBSD phase and orientation. In this case, as the meteorite features both extremely large and fine-scale microstructural features, a multi-scale approach is likely the best.

Conclusion

The application of correlative mechanical microscopy with EDS and EBSD was successfully demonstrated on a fragment of the Seymchan meteorite. All the major features of the investigated area were successfully determined in terms of mechanical properties, orientation, and composition. This was achieved by developing a new open-source python library 'PyXC', which can perform correlation on nearly any 2D datasets. Using displacement-controlled indentations allowed consistent sampling from both mechanical and analytically sampled volumes. Application of this combined correlative approach highlighted challenges within the data. Particularly, the multiple length scales within the meteorite's microstructure suggests that a multi-scale mapping approach would be useful for investigating properties within the coarse and fine-scale microstructural regions. This would not have been apparent by considering the quality of the indentation or EDS maps alone. By visually comparing correlated maps from the various techniques, the causes of local property variations can often be directly ascertained, such as the correlation between decreases in modulus and increased Ni concentration. For general trends and phase level properties, correlated statistical datasets clearly illustrate trends between indentation mechanical property clusters and orientation and compositional trends. This demonstrates the potential of this new correlative approach for future investigations.

Acknowledgements

This work was performed in collaboration with the Prof. Sandra Korte-Kerzel's group at the Institut für Metallkunde und Materialphysik, RWTH Aachen University. Additional details on this work are available in an open-access publication in *Materials & Design*:

Seehaus, S.-H. Lee, T. Stollenwerk, J.M. Wheeler, S. Korte-Kerzel. Estimation of directional single crystal elastic properties from nano-indentation by correlation with EBSD and first-principle calculations, Materials & Design 234 (2023) 112296.

References

1. J.M. Wheeler, B. Gan, R. Spolenak, *Small Methods*, 6 (2022) 2101084.
2. C.M. Magazzeni, H.M. Gardner, I. Howe, P. Gopon, J.C. Waite, D. Rugg, D.E. Armstrong, A.J. Wilkinson, *Journal of Materials Research*,

- 36 (2021) 2235-2250.
3. H. Besharatloo, J.M. Wheeler, *Journal of Materials Research*, 36 (2021) 2198-2212.
 4. F. Bachmann, R. Hielscher, H. Schaeben, *Solid state phenomena*, 160 (2010) 63-68.
 5. W.C. Oliver, G.M. Pharr, *Journal of Materials Research*, 7 (1992) 1564-1583.
 6. P.S. Phani, W. Oliver, *Materials & Design*, 164 (2019) 107563.
 7. M. Seehaus, S.-H. Lee, T. Stollenwerk, J.M. Wheeler, S. Korte-Kerzel, *Materials & Design*, 234 (2023) 112296.
 8. J.M. Wheeler, *Journal of Materials Research*, 36 (2021) 94-104.